Parameters Affecting Orthogonal SAR Transmit and Receive Module Calibration

Daniel Bast

European Space and Technology Centre, European Space Agency

EOP-FI, Keplerlaan-1, 2200 AG Noordwijk (The Netherlands)

E-mail: Daniel.Bast@esa.int

1 Abstract

A novel calibration method has been proposed whereby the complete signal path for each transmit and receive module (TRM) is characterized during imaging-like conditions. This characterization includes components normally contained within an internal calibration loop as well as the actual transmitting elements. The method utilizes the selectable phase and gain settings in each TRM normally used for focussing antenna beam-patterns. Each signal burst independently switches these TRM settings according to an orthogonal code sequence. During post-processing, the recorded data is decoded using the inverse orthogonal sequence to recover the individual TRM characteristics. With this method, it is possible to fully characterize the TRMs without the standard requirements of an external reference signal and/or an internal calibration loop.

This paper illustrates problems associated with the removal of these two aids and how they are overcome. Specific problem areas such as oscillator and TRM stability are explored. Theoretical and simulated results are included to illustrate how these errors affect characterization. One solution is the use of an iterative algorithm to minimize these errors.

2 Introduction

Calibration of data acquired through the use of a phased array antenna requires accurate beam-pattern corrections. These corrections are calculated based on characterization data for each transmit/receive module (TRM). In some current and future SAR systems, such as ESA's proposed TerraSAR-L, each of these TRMs has various settings (u) for phase delay (d_u) and gain attenuation (g_u), see Figure 1. Specifically, TerraSAR-L has 140 TRMs, each of which has individual 6-bit phase shifters and gain attenuators. These produce a phase range of 0 to 360° with a resolution of 5.625° and an attenuation range of 0 to $-$ 31.5 dB with a resolution of 0.5 dB. It is expected only 4-bits will be used to control gain.

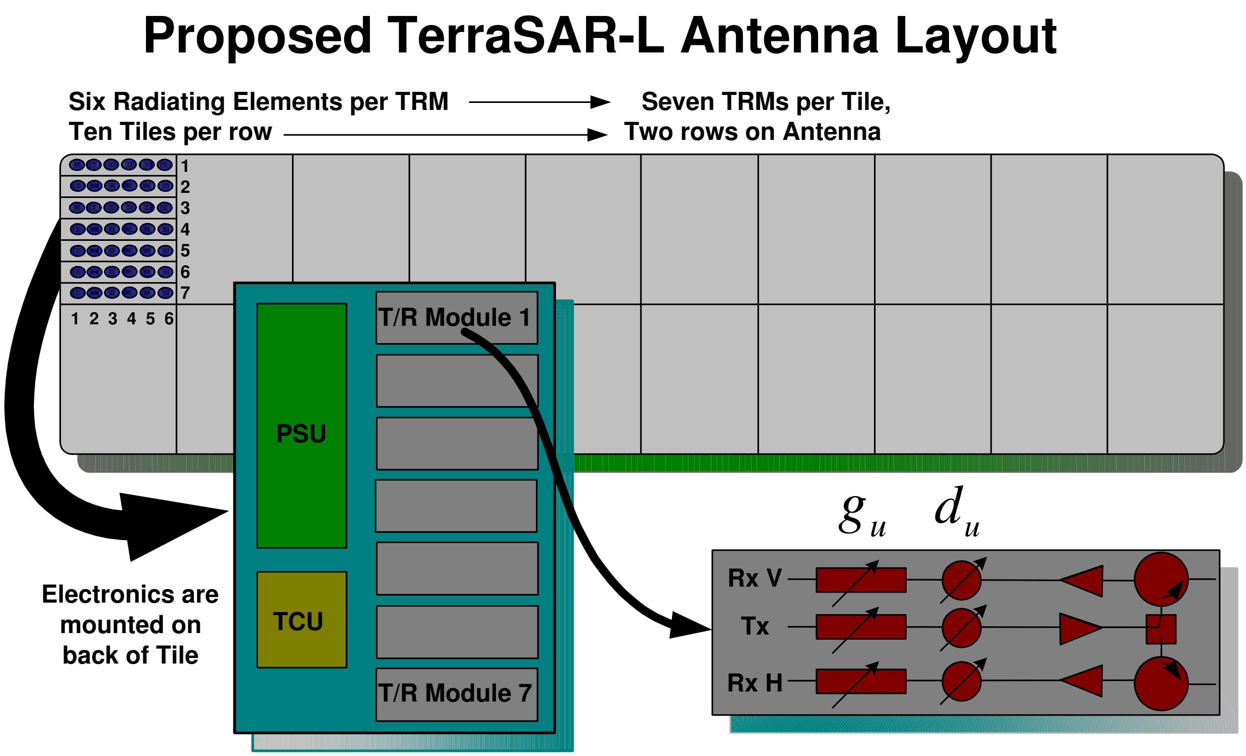

Figure 1: Example of Phased Array Antenna as Proposed for ESA's TerraSAR-L

This paper presents results using design details from TerraSAR-L; however, the algorithms given are generic in nature and can be easily transferred to any phased-array system, including non-electromagnetic wave systems such as sonar. The implementation of orthogonal coding on TerraSAR-L has been termed "Pulse Coded Calibration" or PCC.

3 Orthogonal Coding Theory (Silverstein PCC)

Orthogonal coding as proposed by Silverstein [1] and Purdy [2] activates the largest phase shifter in each of the TRMs according to an orthogonal sequence. A short RF burst is transmitted for each code in the sequence. This process effectively creates a series of pseudo-random antenna patterns that are detected at a remote location. The inverse orthogonal sequence is then used to determine the characteristics of the individual TRMs. It is important to note that during this process all the TRMs transmit simultaneously as in regular imaging. However, the phase settings of each TRM change independently for each burst.

A Hadarmard matrix H is chosen as the orthogonal sequence and produces two encoding matrices, an F and an R code given as D^F and D^R, respectively. The F code uses all the -1's to activate the encoding shifter while the R code uses the $+1$'s. Silverstein's main equation is given as (1)

$$D^F - D^R = H(I - D_u) \tag{1}$$

where I is the identity matrix and D_u is a matrix with d_u arranged along the diagonal. Equation (1) is followed by (2) and (3) with S as the straight through paths (i.e. no shifters or attenuators).

$$\begin{aligned} D^F S - D^R S &= H(I - D_u)S & (2) \\ H^{-1}(D^F S - D^R S) &= H^{-1}H(I - D_u)S \\ &= (1 - d_u(n))S(n) & (3) \end{aligned}$$

where the (n) indicates vector index. With the u^{th} phase shifter activated as the encoding shifter, the matrix inversion produces the following two vectors for the cases where a) no other phase shifter is activated, and b) the v^{th} shifter is activated in all TRMs as given by (4) and (5), respectively. This allows the determination of the v^{th} shifters by taking the ratio of (5) and (4) as shown in (6).

$$\begin{aligned} Z_u(n) &= (1 - d_u(n))S(n) & (4) \\ Z_{uv}(n) &= (1 - d_u(n))d_v(n)S(n) & (5) \\ d_v(n) &= \frac{Z_{uv}(n)}{Z_u(n)} & (6) \end{aligned}$$

The reader is directed to Silverstein [2] for a more detailed explanation of the process.

4 Error Variance Model

Overall, the process is dependent on the accurate and coherent detection of each signal burst. Silverstein accomplishes this by transmitting a separate coherent reference signal to the remote location. However, for TerraSAR-L this presents additional hardware challenges as the design does not call for simultaneous transmission of both the radar and communication sub-systems. Also, the reverse paths are required in order to measure the receive hardware. Thus, a method of implementing a PCC scheme that simultaneously measures both transmit and receive paths without the use of a coherent reference signal has been developed [3].

This new algorithm takes advantage of the statistical averaging during the decoding process to remove errors present in the encoded data. As the removal of the coherent reference signal does not allow coherent detection of the calibration signal, it can be assumed that most of the error is phase related. Thus, a phase error matrix given as:

$$E^F = \begin{bmatrix} e^F_{11} & e^F_{12} & \cdots & e^F_{1N} \\ e^F_{21} & e^F_{22} & \cdots & e^F_{2N} \\ \vdots & \vdots & \ddots & \vdots \\ e^F_{N1} & e^F_{N2} & \cdots & e^F_{NN} \end{bmatrix} \quad (7)$$

for the F code and a separate matrix for the R code is added to the angle of the encoded matrix D^F and D^R in (8), respectively.

$$\theta = D^F + E^F \quad \text{and} \quad \beta = D^R + E^R \quad (8)$$

where it is also assumed $|D^F| = |D^R|$. Trigonometric identities can be used to re-write (1) with θ and β to give (9).

$$e^{j\theta} - e^{j\beta} = |2\cos([\theta - \beta - \pi]/2)|\, e^{j(\theta+\beta+\pi)/2} \quad (9)$$

Re-substitution allows the magnitude and phase terms to be separated in (10)

$$
\begin{aligned}
e^{j\theta} - e^{j\beta} &= \left|2\cos\left(\left[(D^F - D^R) + (E^F - E^R) - \pi\right]/2\right)\right| && \text{Magnitude} \\
&\times \; e^{j(D^F+D^R+\pi)/2} && \text{Encoding Phase} \\
&\times \; e^{j(E^F+E^R+\pi)/2} && \text{Error Phase}
\end{aligned} \tag{10}
$$

The ratio taken in (6) also applies to (10). Thus, phase variance for the v^{th} shifters are given as (11).

$$
\begin{aligned}
\text{Var } d_v^{err} &= \text{Var } \angle \left(e_{uv}^{j(E^F+E^R+\pi)/2} \div e_u^{j(E^F+E^R+\pi)/2} \right) \\
&= \text{Var} \left(\frac{(E^F+E^R)_{uv} - (E^F+E^R)_u}{2} \right)
\end{aligned} \tag{11}
$$

where the subscripts $_{uv}$ and $_u$ are used to denote the different error matrices for both cases.

The error matrix given in (7) is a combination of all possible phase errors. Figure 2 illustrates two mechanisms that combine to create an error matrix based on a simple transmit only antenna with four TRMs (six elements each). In this example, one type of phase error is set to $e_1^{Osc} = 2°$ for all TRMs on the 1$^{\text{st}}$ pulse (denoted by the 1$^{\text{st}}$ subscript = 1). In this case, a 2° error is a result of a phase delay in the RF signal oscillator that is not known by the remote receiver (as it is not coherent with the local oscillator). The 2$^{\text{nd}}$ pulse, $e_2^{Osc} = -1°$, has a different phase error of $-1°$ and so on, for all N pulses.

The next type of phase error is $e_{1j}^d = [+3°, -2°, ..., -5°]$ occurs independently in each of the $j = 1$ to 4 TRMs. It is due to the phase instability of each phase shifter, i.e. the four shifters have nominal values of 180° but actually produce $[183°, 178°, ..., 175°] \Rightarrow e_{1j}^d = [+3°, -2°, ..., -5°]$. These errors vary between pulses, i.e. $e_{2j}^d = [+4°, -1°, ..., -4°]$

Thus, these two errors combine to produce a single phase error matrix in (12).

$$
\begin{bmatrix} +2 & +2 & \dots & +2 \\ -1 & -1 & \dots & -1 \\ \vdots & \vdots & \ddots & \vdots \\ X & X & \dots & X \end{bmatrix} + \begin{bmatrix} +3 & -2 & \dots & -5 \\ +4 & -1 & \dots & -4 \\ \vdots & \vdots & \ddots & \vdots \\ Y & Y & \dots & Y \end{bmatrix} = \begin{bmatrix} +5 & 0 & \dots & -3 \\ +3 & -2 & \dots & -5 \\ \vdots & \vdots & \ddots & \vdots \\ X+Y & X+Y & \dots & X+Y \end{bmatrix} \tag{12}
$$

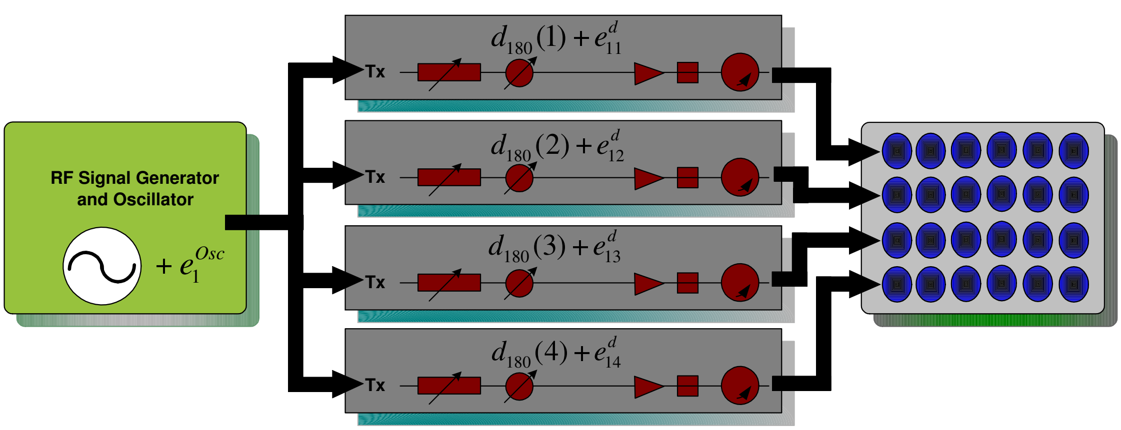

Figure 2: Illustration of two types of Phase Error: a) RF oscillator error and b) Phase Shifter Instability

5 Effects of Errors on PCC

Although Figure 2 was based on two types of phase errors, the final error matrix will include all possible sources of phase error. It is important to note that errors that vary within one row (row-based errors) represent variations between TRMs within a single pulse (usually internal to the TRM) while column-based errors represent variations between pulses (usually external to the TRM).

Column-based phase errors include such parameters as atmospheric/target variations, range to target variations, oscillator/signal generation stability, non-coherent reception, quantization and signal sampling orthogonality, etc. Row-based phase errors include TRM stability, mutual coupling between modules (MCM), path leakage, temperature variation, impedance mismatches, etc.

Figures 3 and 4 illustrate the effect of these errors with comparison to single element (SE) measurements. Figure 3 incorporates row based phase and gain instability. Figure 4 focuses on the straight through paths S and adds a column based phase variation.

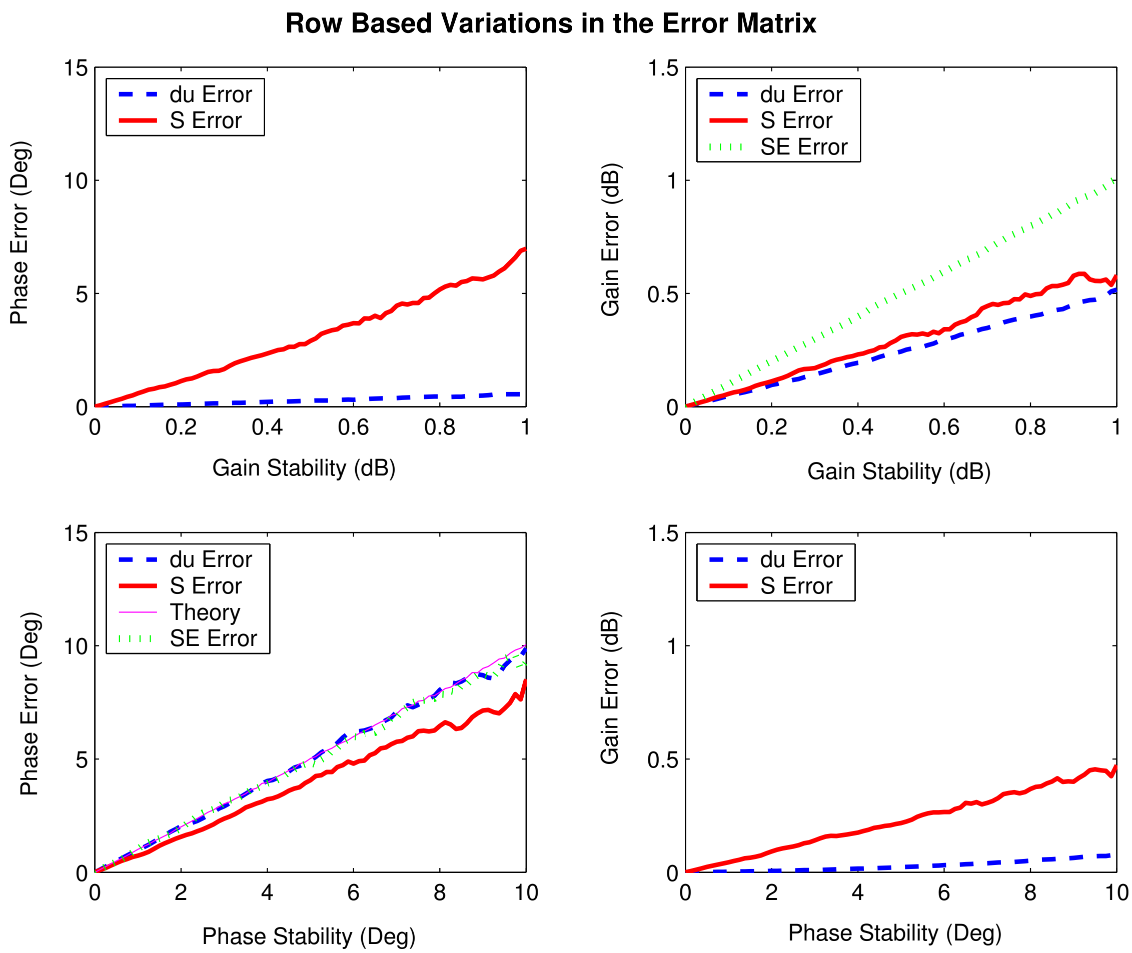

Figure 3: Results of Phase Shifter Instability

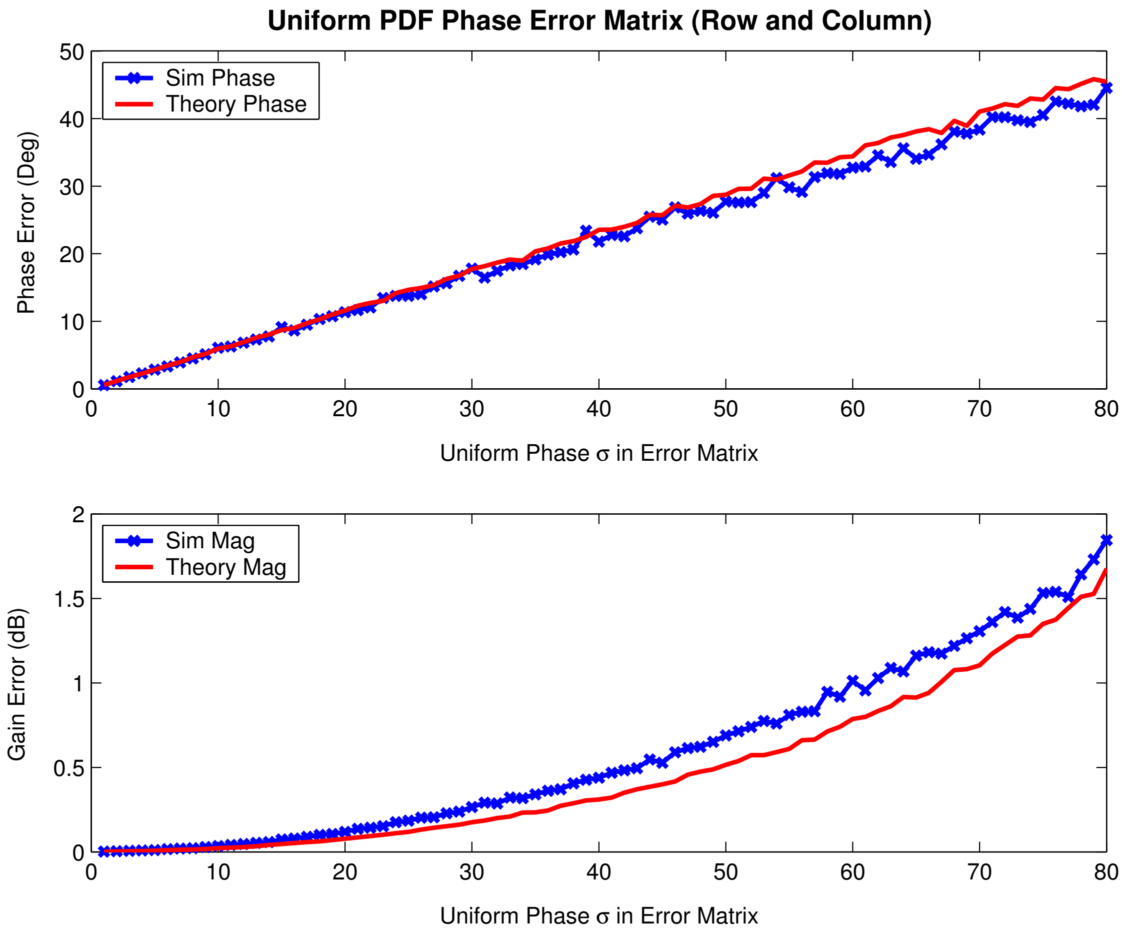

Figure 4: Phase error matrix with uniform PDF due to: a) RF hardware delay and b) Phase Shifter Instability

6 Non-Coherent Iterative PCC

The algorithms given in Bast [3] solve for column based errors while the original Silverstein equations they incorporate yield estimates based on variations within a row. Silverstein's use of a coherent reference signal was intended to account for column based errors. It was also stated in [3] that Gaussian distributed phase erros were required for convergence. Further simulation and the basic model in (11) have illustrated that convergence is not limited to Gaussian cases. The central limit theorem is used as a minimum of four separate error matrices are involved. Thus, as long the combination of the matrices in (11) yield a Gaussian PDF the algorithms in [3] converge. Simulations with four uniformly distributed matrices from L-Band airborne data have shown that (11) tends to a Gaussian PDF, especially as N increases (i.e. $N > 32$).

A brief summary of the most relevant portion from Bast [3] explains how the variance of these error matrices is reduced to a minimum such that the absence of a coherent reference signal is accounted for.

1. Range phase/power variations corrected by curve fitting and GPS data.

2. Atmosphere phase/power variations corrected by curve fitting and atmospheric modeling. Steps 1) and 2) help ensure error matrix is zero-mean.

3. Constrained iterative algorithm corrects for remaining column based errors by:

   (a) Estimate encoded antenna patterns with old TRM estimates and remove from signal data.

   (b) Add Gaussian phase noise to this new data to estimate column based phase noise.

   (c) Remove phase noise from original signal data.

   (d) Decode via Silverstein to produce new TRM estimates.

   (e) Constrain/weight new TRM estimates within reasonable limits.

   (f) Incorporate new TRM estimates back into step a) or even 1).

The convergence limit is based on the accuracy of the beam-pattern equations and a priori TRM characterization data. Typically, the beam equations are used to determine the magnitude of the beam-patterns and not its overall phase. Thus, sufficient antenna ground testing and modeling are imperative such that both the magnitude and phase of the the antenna patterns can be accurately predicted (accuracy within 1 dB and 40°).

Although there are large initial phase errors, the iterative algorithm reduces the phase variance by combining the decoded signal data with a prior TRM characterization knowledge to estimate this column based error (via the antenna equations). Each iteration subsequently improves this estimate leading to more accurate TRM data for the next iteration. Overall accuracy is limited by row based errors (which also limits SE measurements) and antenna equation accuracy.

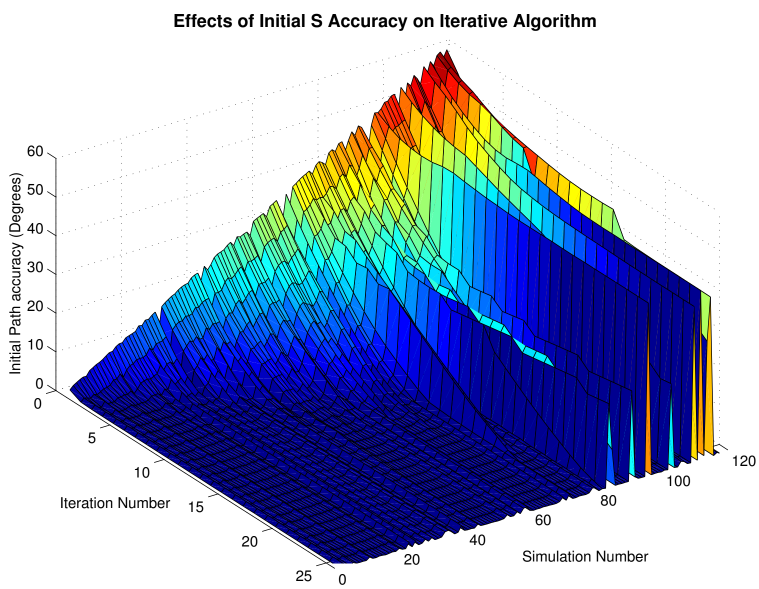

Figure 5: Column based phase errors solved by iterative algorithm

An interesting point to understand from this analysis is that phase information is not required from the received data (although accurate phase data reduces the required number of iterations). During the iterative process, steps b) and c) can be replaced by adding small amounts of random computer generated phase data to the estimated antenna patterns in a).

The added phase noise is used solely to ensure a difference in the forward and backwards matrix inversions. Inaccurate antenna equations will require less added phase noise than accurate equations. If the antenna equations were perfect and no phase noise was added, then the resulting inversion would produce exactly the same TRM data as was used when calculating the equations. The algorithm would not converge since the equations are the same. However, this is unlikely as most equations predict antenna patterns within 0.5 dB and 20° or so.

7 Conclusion

Error parameters affecting orthogonal TRM characterization have been modeled and simulated in various configurations. Results from the iterative PCC algorithm indicated that unknown phase variations between pulses can be successfully corrected. Overall accuracy is limited by TRM stability and the accuracy of the antenna beam-pattern equations employed. Based on these results, PCC will prove a useful tool in characterizing the complete RF chain in most phased array antennas.

Work is ongoing in developing laboratory experiments to verify the iterative algorithm. This algorithm is also being modified to correct for radiometric variations due to Nadir target reflections. Current results indicate that without iterative correction, targets must be radiometrically stable within approximately 0.5 dB. Further work will improve this limit.

References

[1] Silverstein, S D. *Application of orthogonal codes to the calibration of active phased array antennas for communications satellites*. IEEE Trans. Sig. Proc., Vol 45, No 1, January 1997.

[2] PURDY, D S. *In orbit active array calibration for NASA' s LightSAR*. Proceedings of the 1999 IEEE Radar Conference, pp172-176, April 1999

[3] Bast, D.C. *A Pulse Coded Calibration Scheme for SAR Antennas*. EUSAR 2004, 25-26 May, Ulm, Germany.